Journal of Ayurveda and Integrative Medicine 11 (2020) 24–36

Contents lists available at ScienceDirect

Journal of Ayurveda and Integrative Medicine

journal homepage: http://elsevier.com/locate/jaim

Original research article (experimental)

Improved drug carriage and protective potential against Cisplatin-induced toxicity using Boldine-loaded PLGA nanoparticles

Jesmin Mondal [a], Mousumi Patra [b], Ashis Kumar Panigrahi [c], Anisur Rahman Khuda-Bukhsh [a, *]

[a] Cytogenetics and Molecular Biology Laboratory, Department of Zoology, University of Kalyani, Kalyani 741235, India
[b] Molecular Biology Laboratory, Department of Biochemistry and Biophysics, University of Kalyani, Kalyani 741235, India
[c] Fisheries and Aquaculture Laboratory, Department of Zoology, University of Kalyani, Kalyani 741235, India

ARTICLE INFO

Article history:
Received 7 June 2017
Received in revised form
6 September 2017
Accepted 14 November 2017
Available online 14 August 2018

Keywords:
PLGA-nano-encapsulation
Boldine
Cisplatin
Multiorgan-toxicity
DNA-targeting
Signalling-pathway

ABSTRACT

Background: Cisplatin is a widely-used potent anti-cancer drug having severe side-effects precluding its sustained use.
Objectives: Poly (lactide-co-glycolide) (PLGA)-nanoparticles loaded Boldine, an antioxidant ingredient of ethanolic extract of Boldo plant (*Peumus boldus*) was tested in cancer mice model, *Mus musculus* to examine if it could reduce unwanted Cisplatin-induced toxicity in normal tissue.
Material and methods: Nano-encapsulation of Boldine was done by following the standardized solvent displacement method. Physico-chemical characterization of PLGA-encapsulated nano-Boldine (NBol) was accomplished through analyses of various spectroscopic techniques. Status of major antioxidant enzymes, functional markers, and lipid peroxidation (LPO) was also determined in certain tissue and serum samples. Percentage of cells undergoing cytotoxic death, Reactive oxygen species (ROS) accumulation and mitochondrial functioning were analyzed in both normal and cancer mice. Nanoscale changes in chromatin organization were assessed by Transmission electron microscopy (TEM). mRNA and protein expressions of Top II, Bax, Bcl-2, Cyt *c*, caspase 3 were studied by RT-PCR, immunoblot and immunofluorescence.
Results: NBol had faster mobility, site-specific action and ability of sustained particle release. NBol readily entered cells, prevented Cisplatin to intercalate with dsDNA resulting in reduction of chromatin condensation, with corresponding changes in ROS levels, mitochondrial functioning and antioxidant enzyme activities, leading to reduction in Deoxyribose nucleic acid (DNA) damage and cytotoxic cell death. Expression pattern of apoptotic genes like Top II, p53, Bax, Bcl-2, cytochrome *c* and caspase-3 suggested greater cytoprotective potentials of NBol in normal tissues.
Conclusions: Compared to Boldine (Bol), NBol had better ability of drug carriage and protective potentials (29.00% approximately) against Cisplatin-induced toxicity. Combinational therapeutic use of PLGA-NBol can reduce unwanted Cisplatin-induced cellular toxicity facilitating use of Cisplatin.

1. Introduction

Cisplatin [cis-diamminedichloroplatinum (II)], an alkylating agent, is a very efficient chemotherapy drug that is used widely to treat different cancers including testicular, cervical, head, neck, bladder and lung cancer [1]. Despite being a potent anticancer drug, clinical use of this agent is limited predominantly because of its strong side-effects on various organs like kidney, liver, brain and gastrointestinal tracts [2–4]. Once Cisplatin is transported into cells, the chloride ions dissociate from the positively charged platinum ion which bind to cellular Deoxyribose nucleic acid (DNA), RNA and proteins [5], and inhibit replication, transcription, translation and DNA-repairing [6]. Because of its inhibition of antioxidant enzymes and proteins, major side effects like nephrotoxicity and hepatotoxicity [7,8] are produced. Nitric oxide plays an important role in Cisplatin-induced nephrotoxicity along with

* Corresponding author.
E-mail: prof_arkb@yahoo.co.in
Peer review under responsibility of Transdisciplinary University, Bangalore.

https://doi.org/10.1016/j.jaim.2017.11.002

other Reactive oxygen species (ROS) such as superoxide anion and hydrogen peroxide [9]. Another main reason for Cisplatin-induced toxicity possibly could be due to depletion of reduced glutathione (GSH) [10]. It has also been reported that both p53 dependent expression of caspases-cascade and p53-independent activation of caspases [11] through Bax/Bcl2 mediated release of cytochrome C contribute to Cisplatin induced cellular death [12]. Patients treated for cancer with platinum-based compounds frequently develop cognitive impairment and structural abnormalities in the brain [13]. Therefore, one of the major objectives of this study was to examine if co-administration of Boldine (Bol) or nano-Boldine (NBol) with Cisplatin could have some protective effect against Cisplatin-induced toxicity in normal cells but without having such protective effect against Cisplatin-induced toxicity in cancer cells.

Bol, the major leaf and bark alkaloid of the Chilean boldo tree *(Peumus boldus)*, chemically known as (S)-2, 9-Dihydroxy-1, 10-dimethoxy-aporphine, has been shown to behave as a potent antioxidant. The ethanolic crude extract of Boldo plant is generally used as a homoeopathic drug against severe liver toxicity related disorder. The major biologically active ingredient, Bol, shows pharmacological activities like cyto-protective, anti-tumour and protective effect against neuronal damage [14,15]. However in recent years nanoparticles of biodegradable non-toxic polymers, harmless to target organism, are preferred as carriers because of their high drug-loading capacity, controlled drug release and lack of requirement of surgical intervention for removal of depleted drug [16]. Poly (lactide-co-glycolide) (PLGA)-based nanoparticles delivery has many advantages like non-degradable and sustained release of the therapeutic agent [17,18]. Moreover, due to their smaller size, nanoparticles can penetrate specific tissues via receptors over-expressed by target cells or the blood brain barrier [19,20]. Another major advantage of PLGA over other polymers is that it can improve pharmacokinetic and pharmacodynamic profiles and is approved by the FDA and EMA in various drug delivery systems.

In our earlier studies [21,22], we demonstrated that conjoint use of a low dose of boldo plant extract could reduce Cisplatin-induced cytotoxicity in normal cells but did not affect much its cytotoxic effect in cancer cells *in vitro*; however, its similar effects, if any, had not been tested in any mammalian model *in vivo*.

Therefore, the main objectives were whether: i) encapsulated Boldine (Bol) would show better potentials of reducing Cisplatin-induced cytotoxicity in normal cells at a reduced dose than un-encapsulated Bol, ii) to determine bio-distribution of Bol and NBol in different tissues of mice including their ability to cross blood–brain barrier, iv) to evaluate their relative ability to scavenge highly reactive free radicals as effective antioxidant, and v) to address the molecular mechanism of action, particularly in respect of the cytotoxicity signalling responses triggered by NBol vis-à-vis un-encapsulated Bol.

2. Materials and methods

2.1. Reagents

All the chemicals used in this study were of analytical grade and procured from Sigma Chemical Co., St. Louis, MO, USA.

2.2. Preparation of blank and drug loaded nanoparticles

PLGA-encapsulated NBol were prepared using a one-step procedure of nanoprecipitation, also known as the solvent displacement method [23] described elsewhere [22]. The nanoparticle-loaded suspensions thus prepared were stored at 4 °C until use. For blank nano-particles, the same method was set up without the addition of Bol.

2.3. Characterization of NBol

The size of the nanoparticles of Bol was earlier determined [22] to be 115.5 ± 0.469 nm, and zeta potential to e (−) 17.4 ± 2.38 mV, with % of yield as 84.19 + 1.72, encapsulation efficiency of 81.93 ± 0,915% and polydispersity index of 0.217 ± 0.016.

2.3.1. UV–vis spectrophotometry

UV–vis spectrophotometric data reported here were all obtained by using a Shimadzu 1800 UV–vis spectrophotometer. The supernatant containing nanoparticles (NBol) was used for spectroscopic scan analysis in the wavelength region of 220–800 nm.

2.3.2. Fluorimetry

Fluorescence emission spectra between 400 and 600 nm was recorded using a fluorescence spectrophotometer equipped with a xenon lamp. The excitation wavelength was set at 310 nm.

2.3.3. Structural integrity assessment by fourier transform infrared spectroscopy (FTIR)

FTIR gives information about the groups present in that particular compound. FTIR spectra of NBol, bulk Bol and also of blank PLGA nanoparticles were recorded on KBr plates in the scanning range of 400–4000 cm^{-1} and at 1 cm^{-1} resolution using FTIR spectrometer (Perkin Elmer).

2.3.4. Release kinetics of Bol from its encapsulated form

Bol release studies from NBol were performed in PBS solution at pH 7.5. Bol release rate from NBol was determined using the routine dialysis-bag method under sink condition [24].

2.3.5. Tissue distribution assay of Bol and NBol

Amount of distribution of drug in bulk (Bol) and its nanoform was measured in various tissues of mice by relative absorption potentials of Bol and NBol. Mice orally administrated single dose of 10 mg/kg body weight (bw) of blank PLGA nanoparticles group, Bol group and NBol group. After 24 hr incubation, mice were sacrificed and tissues of brain, lung, heart, liver, kidneys, spleen and plasma from blood were also analyzed.

2.3.6. Transmission electron microscopic analysis of brain tissue

Brain tissues of mice receiving the dose of 5 mg/kg bw and 10 mg/kg bw of NBol, respectively, were collected at day 7 to analyze whether NBol could cross blood brain barrier. Tissue was fixed in 2% paraformaldehyde, 2.5% glutaraldehyde and in 1% osmium tetroxide solution, dehydrated in a graded series of ethanol, and embedded in Epon resin. 1% uranyl acetate stained ultra-thin sections were observed under Transmission electron microscopy (TEM) with a Tecnai G2 electron microscope operating at 200 kV.

2.3.7. Circular dichroism (CD) and UV spectral analysis

Changes in CD signals were noted for known amount of ctDNA alone, then after addition of Cisplatin, and then after addition of either Bol or NBol in equal amount. Changes which occurred in CD signals of the DNA upon interaction with drugs may often be assigned to corresponding changes in the normal B-form CT-DNA in the region (200–450 nm). Rectangular quartz cuvette (Jasco Spectropolarimeter; model PC controlled J-815; Jasco International Co. Ltd. with a temperature controller and thermal programmer PFO 425L/15) with 1 cm path length was used at 37 °C temperature.

Alteration of UV spectra of CT (Calf Thymus) DNA (260 nm) with stepwise addition of Bol was recorded at three different temperatures, 293 K, 303 K and 313 K, respectively, using a Shimadzu (UV160-A) spectrophotometer. NBol was added in both the sample and reference cuvettes for eliminating scattering of NBol. Strength and nature of NBol binding to DNA was determined by analysis of absorbance data, using the Hill equation. The complexation between CT-DNA and NBol was determined by analyzing thermodynamic parameters ΔH (change in enthalpy) and ΔS (change in entropy) which could be easily calculated from the binding constant at those temperatures at 293, 303 and 313 K through Van't Hoff equation. Putting values of ΔH and ΔS to the standard thermodynamic equation $\Delta G = \Delta H - T\Delta S$, value of ΔG (change in free energy) of the interaction was determined [25] [see Supplementary data file 5 for detailed methodological procedure].

2.4. Animals

Healthy swiss albino mice (*Mus musculus*) of both sexes, weighing 20–25 gm, were acclimatized in an environmentally controlled room (humidity, 55 ± 5%, temperature, 24–26 ± 2 °C; 12-h light/dark cycle) for at least 14 days with access to food and water *ad libitum*, and used as experimental materials. We followed experimental protocols duly approved by Institutional Ethics Committee, University of Kalyani, and under supervision of Animal Welfare Committee, University of Kalyani. (Vide: Certificate for Proposal No. KU/IAEC/Z-11/07, dated 18.5.2007.)

2.5. Induction of cancer in normal mice

Bezo[a]pyrene (BaP) (50 mg/kg bw) suspended in olive oil, was administered orally twice a week to normal healthy mice for one month and then they were kept on a normal diet for three more months for onset and development of hepato-cellular carcinoma.

2.6. Dose selection for Cisplatin

Cisplatin was administered intraperitoneally (IP) at a dose of 5–30 mg/kg bw. twice a week for one month [26] in mice carrying induced hepatocarcinoma. As Cisplatin treatment at the concentration of 10 mg/kg bw. apparently gave the best protective effects on liver cancer (Supplementary data 1), normal healthy mice were treated with Cisplatin at that concentration (10 mg/kg bw) to examine if this could have any toxic effect on normal healthy mice. Toxicity level was measured in different organs of mice before and after Cisplatin treatment by means of critically observing tissue histology and quantity of Lactate dehydrogenase (LDH) in mice (Supplementary data 2).

2.7. Selection of dose for Bol and NBol

Normal healthy mice with induced liver cancer were orally administrated with optimum dose of 10 mg/kg bw Bol/NBol once daily for 30 consecutive days, to examine individual effect of Bol/NBol, if any, on normal and cancer mice (Supplementary data 3) sacrificed after 1 more month, when they received no more drugs.

2.8. Experimental design

24 mice (20–25 gm bw) were randomly selected and divided into 4 groups, each with 6 mice for further experiments.

Group 1 Negative control: 6 out of 24 mice were fed normal diet and water *ad libitum*. Mice were injected (i.p.) with PBS (6.6 mL/kg bw) twice a week for 1 month.

Group 2 Cisplatin control: Cisplatin i.p. was injected to remaining 18 mice at a dose of 10 mg/kg bw twice a week for one month which served as hepatotoxic positive control group.
Group 3 Bol treated sub-group: Boldine (10 mg/kg bw) was fed to a subgroup of six mice from group 2 (i.e. six mice from group of 18 mice fed with Cisplatin) hepatotoxic mice.
Group 4 NBol-treated subgroup: NBol (10 mg/kg bw) was fed to a subgroup of six mice from group 2 (i.e. six mice from group of 18 mice fed with Cisplatin) liver intoxicated mice.

2.9. Cytotoxicity determination

Cytotoxic effects of Bol and NBol in normal groups of mice were determined by removing liver tissue aseptically and perfusing it in dulbecco's modified eagle's medium (DMEM). The cell suspension was incubated at 37 °C and Thiazolyl blue tetrazolium bromide (MTT) assay was performed [27].

2.10. Histopathology

Liver and kidney tissues of normal mice and liver of induced-cancer mice were fixed by immersion in 10% neutral buffered formalin for 3 day at room temperature. Fixed tissues were routinely processed into paraffin-wax blocks, sectioned and stained with hematoxylin-eosin (HE) and observed under light microscope (Leica, Germany).

2.11. Biochemical analysis of enzymatic parameters

We analyzed serum levels of creatinine and blood urea nitrogen using commercially available kits provided by Span Diagnostics, India. We assayed activities of lipid peroxidation (LPO) [28], GSH [29] and superoxide dismutase (SOD) by the standard protocols [30]. We also measured aspartate aminotransferase (AST) and alanine aminotransferase (ALT) using a standardized kit from Liquid Gold Ltd, B.No. LG021, 76LS200-60 and 77LS200-60 [31] following manufacturer's instructions.

2.12. Flow cytometric analysis of early and late apoptosis by Annexin V-FITC and propidiumiodite (PI) staining

Liver was dissected out quickly from each experimental mouse and washed with phosphate buffer saline (PBS). Liver tissue was then minced into small pieces in DMEM media (Himedia, India) and cells were flushed out gently in the media with the aid of a hypodermic syringe. The media containing cells were passed through a thin nylon mesh (0.22 μm) and the cells were spinned down at 1000 g for 3–4 min. Blood cells were pelleted out and the supernatant containing liver cells was used for Annexin V-FITC/PI assay. The rate of apoptosis in 3×10^7 perfused liver cells/well was assessed by Annexin V FITC/PI dual staining, according to the method of Chakraborty et al. [32]. Externalization of phosphatidylserine (PS) during apoptosis and leakage from necrotic cells were analysed by Annexin V-FITC/PI (Propidium iodide) dual staining using the standard protocol. Cell population was differentiated by flow cytometric assay (Fluorescence-activated cell sorting (FACS) caliber, BD Bioscience).

2.13. Assessment of changes in nuclear organization by tissue TEM study

Nanoscale changes in chromatin organization of all groups of mice were measured by TEM by standard method [33]. Ultra-thin sections of different tissue were stained with 1% uranyl acetate and observed under TEM instrument operating at 200 kV.

2.14. Determination of intracellular ROS

Perfuse liver cells of different treatment groups of normal healthy and induced-cancer mice were incubated for 30 min with DCFH-DA (5 mmol/l) at 37 °C in dark [34]. After incubation samples were analyzed using FL-1 band pass filter on flow cytometer (FACS calibur, BD Bioscience). Each data was analyzed by using Cyflogic v.1.2.1 software.

2.15. Mitochondrial membrane depolarization

Liver cells were isolated from different groups of experimental and control mice and incubated with Rhodamine 123 (5 mmol/l) for 15 min at room temp in dark. Fluorescence intensities were measured using Cyflogic v.1.2.1 software utilizing FL-1 band pass filter in flow cytometer (FACS calibur, BD Bioscience) [34].

2.16. RNA extraction and quantitative reverse transcriptase polymerase chain reaction (RT-PCR) analysis

Total RNA was extracted from liver tissue using Trizol reagent and cDNA was used as a template for polymerase chain reaction (PCR) amplification with the aid of Taq polymerase. Synthetic oligonucleotide primers for reverse transcriptase (RT)–PCR were procured from Chromus Biotech, Bangalore, India. Sequences of the forward and reverse primers used for specific amplifications are provided in Supplementary Data file 4. After PCR amplification, DNA bands were photographed and densitometrically analyzed through Total Lab software (Ultra Lum, USA).

2.17. Immunoblot

Immunoblot analysis was conducted by using anti-cytochrome *c*, anti-bax, anti-bcl-2, anti-p53 and anti-top-II antibodies (Santa Cruz Biotechnology, USA) and anti-cleaved caspases-3 antibodies (BD Bioscience, USA). Alkaline phosphatase was used as conjugated secondary antibody (Sigma, USA) [35]. Band intensities were analyzed using Image J software. Glyceraldehyde 3-phosphate dehydrogenase (GAPDH) served as the housekeeping gene, the expression of which was studied with the aid of anti-GAPDH monoclonal antibody (Santa Cruz Biotechnology, USA).

2.18. Analysis of mitochondrial cytochrome c release

Cells for immunofluorescence analysis were prepared by using Mito-Tracker Red (50 nm) and secondary fluorescent Fluorescein isothiocyanate (FITC) anti-goat antibody (Santa Cruz Biotechnology, USA). For confirmation of localization of cyt *c* in mitochondria and cytosol, control and treated cells were incubated for 24 h with primary antibody (Santa Cruz Biotechnology, USA) at 4 °C overnight and developed with secondary FITC conjugated anti-cyt-c antibody. Finally, cells were observed under confocal microscope (Carl Zeiss LSM 510 META Laser Scanning Microscope).

2.19. Statistical analysis

All experiments were performed in triplicate and expressed as mean ± standard error [SE]. Means of values of all data of three independent experiments were statistically analyzed using one-way ANOVA by post hoc analysis (SPSS Version 20) and individual comparisons were obtained by "Least square division (LSD)" method where $^{*}P < 0.05$ vs. was considered to be statistically significant.

3. Results

3.1. Synthesis and characterization of PLGA encapsulated Boldine nanoparticle (NBol)

3.1.1. Absorbance and fluorescence study

There were two peaks of NBol, a sharp peak at 280 nm and a hump like peak at 302 nm (Fig. 1A). In the fluorescence study, NBol showed a strong emission peak at 375 nm when excited at 310 nm wavelength (Fig. 1B).

3.1.2. FTIR study

The major peaks shown by Bol confirmed the presence of different groups. Bonds between 1400 and 1700 cm^{-1} were due to aromatic C–C stretching. In Bol (Fig. 1C) those peaks were at 1425.08 cm^{-1} and 1633.90 cm^{-1}. Those peaks were slightly shifted to NBol NPs (Fig. 1D) at 1449.81 cm^{-1}, 1626.34 cm^{-1}. Peaks at 1161.24 cm^{-1}, 1265.39 cm^{-1} and 1318.78 cm^{-1} signified the C–N vibrations which were also present in the NBol nanoparticles at 1166.89, 1298.49 and at 1315.54 cm^{-1}, respectively. Peaks at around 3412.31 cm^{-1} and at 2925.05, 2113.25 cm^{-1} in bulk Bol shifted to 3286.15 cm^{-1} and 2922.42, 2115.32 cm^{-1} indicated O–H stretching and C–H stretching, respectively. In NBol peak at 1449.81 cm^{-1} (C=C stretching), 1383.06 cm^{-1} (C–H stretching) and at 1166.89 cm^{-1} (C–N stretching) came from the PLGA (Fig. 1E) which were present at 1449.33, 1384.74 and 1165.08 cm^{-1}, respectively. The results therefore confirmed that the major peaks of bulk Bol were also present in the NBol NPs.

3.1.3. Release kinetics of Bol molecules from its nano-encapsulated form

The initial burst release was followed by a slow and sustained release. About 45% of Bol was released within 8 h. Rapid initial release was normally attributed to the fraction of Bol which was adsorbed on the surface of the NPs. At the second stage, the release of Bol was slower and sustained which may be due to diffusion of the Bol entrapped within the core of the NPs. The cumulative release of Bol was a diffusion controlled process under a physiological condition (pH 7.5) and showed a gradual increase and reached a plateau after 48 h with release of 96.45% of Bol (Fig. 1F).

3.1.4. Interaction of NBol and DNA

Result of UV-absorption spectrophotometric study revealed that the absorbance of DNA at 260 nm was decreased gradually with the increasing addition of Boldine Nps (Fig. 2A), indicating some interaction between DNA and Boldine Nps. Value of the binding constant (K_b) of the interaction, as determined from the Hill plot (Fig. 2B), was 10.232×10^3 M^{-1} at 293 K and that of the Hill coefficient (γ) was 1.6942, implying that nature of DNA–Boldine Nps binding was a positive co-operative interaction. Values of K_b and γ at 303 K and 313 K were 9.616×10^3 M^{-1} and 8.912×10^3 M^{-1}; 1.7522 and 1.8841, respectively. Value of $K_b$was decreased with increasing temperature, which signified gradual weakening of interaction with increase in temperature. Using these values of K_b, values of ΔH (change in enthalpy) and ΔS (change in entropy) of the DNA–Boldine Nps interaction were determined from the van't Hoff equation: $\ln(Kb) = -\Delta H/RT + \Delta S/R$ which suggested van't Hoff plot ($\ln K_b$ vs. $1/T$) to be linear (Fig. 2C). Magnitude of the values of ΔH and ΔS signified that the binding reaction was driven by enthalpy contribution, with a rather small entropy contribution and negative value of ΔH implied that binding interaction was exothermic in nature.

Moreover, values of ΔG (change in free energy) at different temperatures 293 K, 303 K and 313 K, were calculated to be −5.358, −5.498, −5.638 kcal M^{-1}, respectively. Negative values

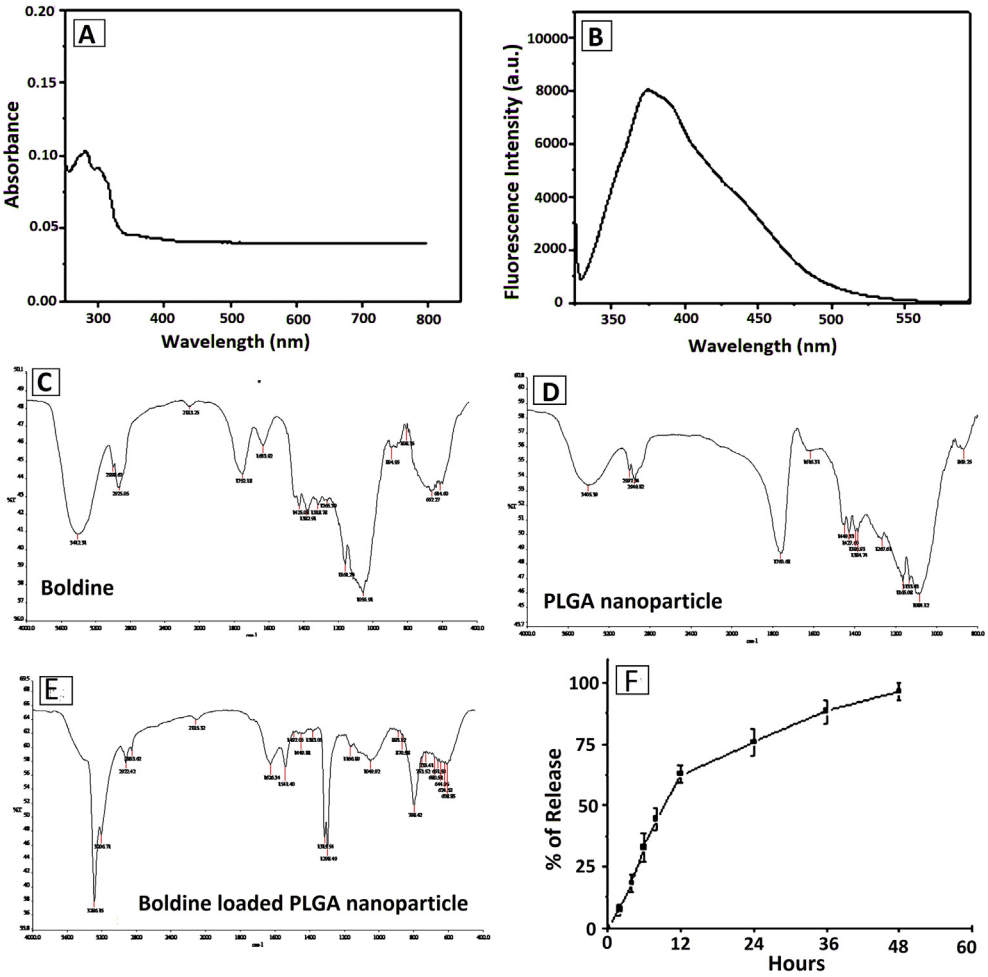

Fig. 1. (A) showing absorbance spectrum and (B) fluorescence spectrum Fourier transformed infrared spectroscopy (FTIR) study of (C) Boldine, (D) blank nano PLGA, (E) PLGA encapsulated Boldine nano-particle and (F) *In vitro* release kinetics of Boldine from nano encapsulation for 72 h time period.

of ΔG (at each temperature) implied that DNA–Boldine Nps binding reaction was a spontaneous phenomenon.

CD spectra (Fig. 2D) of calf-thymus DNA (ct-DNA) consisted of a positive band at 275 nm due to base stacking and a negative band at 245 nm due to its helicity, characteristic of right-handed B form DNA. After adding Cisplatin with ct-DNA, CD spectrum significantly altered with decrease in peak intensity indicating strong interaction. When Bol was added with Cisplatin, the CD spectrum exhibits a slight alteration on both negative and positive absorption intensities without much change in its wavelength, indicating a relatively weak intercalation of drug to ct-DNA. In presence of PLGA encapsulated Boldine NPs (NBol) with Cisplatin, again a significant rise in peak intensities of both bands was observed; this indicates that amount of interaction between Cisplatin and DNA was reduced.

3.1.5. Tissue distribution of Bol and NBol in mice

Percentages of Bol and NBol intensities in all tissues were analyzed and graphically illustrated in Fig. 3A. From these data it is evident that most of the particles were detected in liver at 34.98% (Bol) and 44.52% (NBol), followed by kidney 18.92% (Bol) and 22.24% (NBol), lung 4.64% (Bol) and 8.82% (NBol), brain 0% (Bol) and 17.46% (NBol), heart 8.24% (Bol) and 13.16% (NBol), spleen 2.28% (Bol) and 3.32% (NBol), plasma 7.74% (Bol) and 9.34% (NBol), after 24 h. Therefore, this could possibly indicate that either Bol had significantly poorer distribution profile than NBol or else, the difference could be due to their differential absorption properties. Due to the nano size, NBol showed better tissue distribution profile and were detected in normal mice liver, kidney and brain tissues.

3.1.6. TEM study to detect presence of nano-particles (Nps) in mice brain

Result of TEM study showed that Boldine Nps (NBol) was present in treatment groups of mice brain (marked by arrow). They were increased in a dose-dependent manner in the nucleus (N) of mice brain as compared with the Nps untreated mice (Fig. 3B), presumably due to their smaller size, negative zeta potential and increased concentration gradient. This would clearly suggest the ability of the NBol to cross the blood brain barrier (BBB).

3.2. Structural integrity of kidney and liver in all groups of mice

Cisplatin alone induced liver damage with tissue degeneration, wide spread apoptosis and vacuolizations in healthy mice, co-treatment of Cisplatin and NBol tended to protect structural damages in livers of these mice, showing near normal features (Fig. 4A).

Only Cisplatin also induced histological changes in kidney, as evidenced by the altered architecture with extensive destruction/atrophy of glomerule, damaged tubular structures and dilatation of urinary space of normal healthy mice. Cisplatin plus Bol or NBol group showed protective effects on kidney with improvement in histological picture showing normal structure of glomerule and

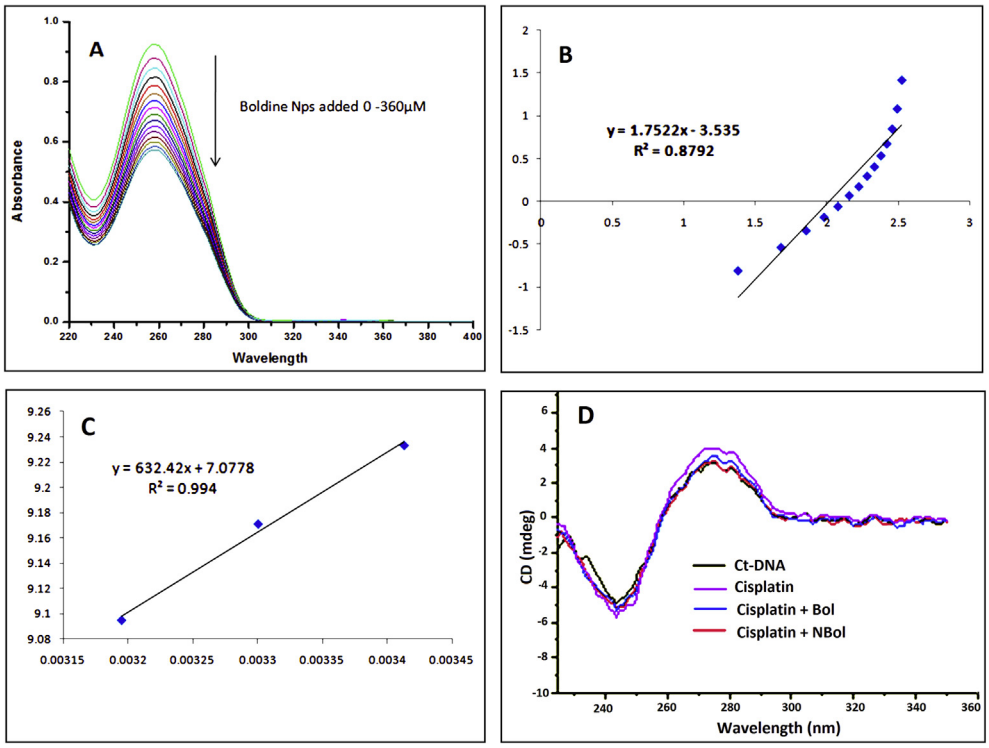

Fig. 2. (A) Changes in UV-absorption spectra of CT DNA with stepwise addition of Boldine NPs (0–360) µM. (B) Hill plot of equilibrium binding between DNA and Boldine NPs. (C) Van't Hoff plot of DNA and Boldine NPs. (D) CD spectral data of DNA-binding ability of Cisplatin alone, Cisplatin + Bol, Cisplatin + NBol.

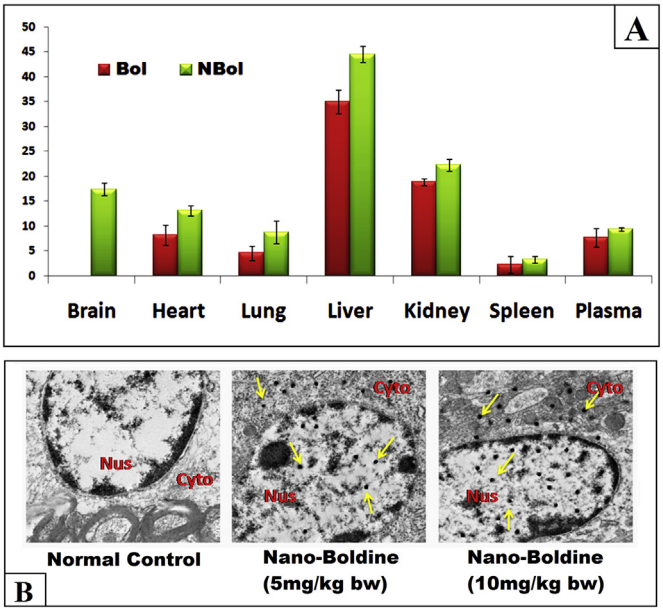

Fig. 3. (A) Tissue distribution of Boldine (Bol) and PLGA encapsulated nano-Boldine (NBol) in different organs. Data are expressed as mean ± SE. (B) TEM of brain tissue showing nanoparticles (Arrowhead marks). Nus-stands for nucleus and Cyto-stands for cytoplasm. Observers were "blinded" during observation and scoring of data.

minimal tubular damage. Better protective features appeared in the Cisplatin plus NBol group (Fig. 4B).

In induced cancer mice, there was extensive damage noted in liver tissue. Treatment with only Cisplatin and Cisplatin plus Bol/NBol showed some recovery effect on liver with improvement of histological structure, showing more or less normal structure of liver hepatocytes (Fig. 4C).

3.3. *Effect of drug treatment on kidney and liver function markers*

Both urea and creatinine levels were higher in the only Cisplatin treated group as compared to control (Fig. 5A). The graph also showed recovery of the markers towards normal levels after combinational treatment with Cisplatin and Bol/NBol. Cisplatin + NBol group showed better recovery result than that of Bol.

Quantification of serum ALT and AST from healthy mice of only Cisplatin treatment group revealed significant increase in these two enzyme levels, indicating elevation of hepatotoxicity. However, when these healthy mice received both Cisplatin and Bol/NBol, appreciable reduction in these enzyme markers was observed, reflecting reduction of liver toxicity as well (Fig. 5B). Serum ALT and AST levels were significantly higher in cancer mice, but the levels appeared to be much less in mice treated with Cisplatin or with the combined therapy of Cisplatin plus Bol/NBol (Fig. 5C).

3.4. *Changes in inter-cellular GSH, SOD and LPO levels in liver and kidney*

When only Cisplatin was administrated to normal mice liver, kidney and brain cells, and increased GSH depletion relative to the control treatment was encountered. Co-treatment of NBol with Cisplatin reduced rates of GSH depletion more strikingly than when compared against the Bol treated with Cisplatin group. In only Cisplatin-treated group, SOD activity was decreased but the co-administration of Bol/NBol with Cisplatin significantly increased the activities of these enzymes towards normal level. When Cisplatin was given to healthy mice, LPO levels increased, indicating the hepatotoxicity and nephrotoxicity expected with this drug. However, when these healthy mice received both Cisplatin and Bol/NBol, enzyme levels were reduced, indicating that toxicity level in both the organs was also reduced (Table 1).

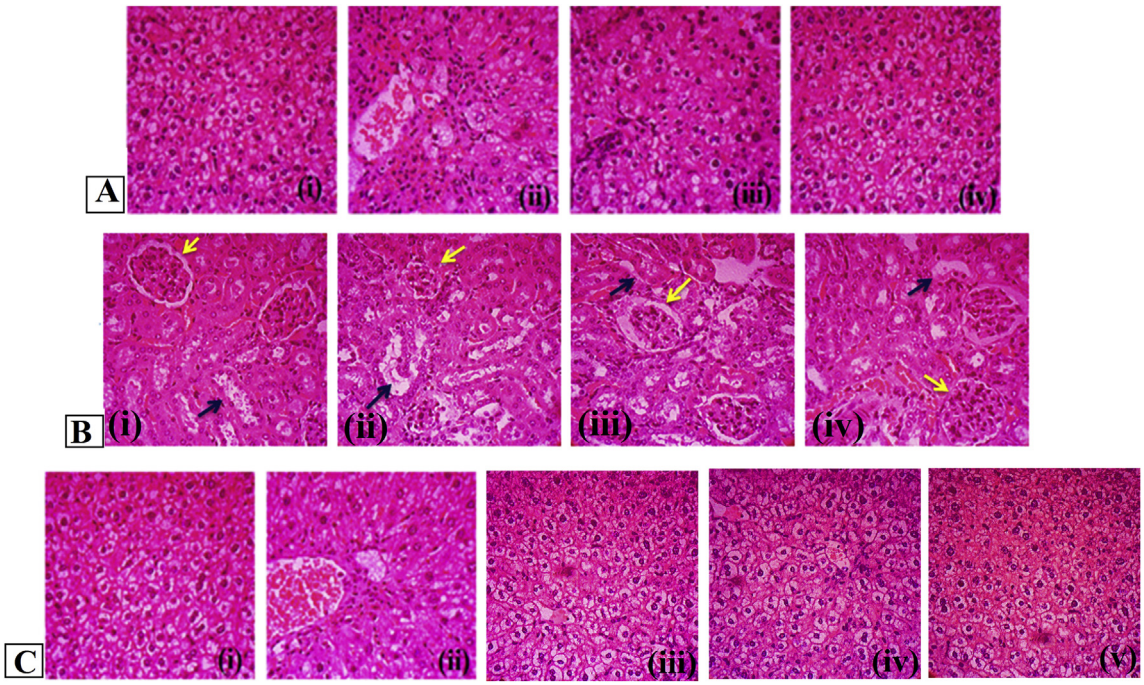

Fig. 4. Histopathology of normal healthy mice liver (A) and kidney (B); Normal mice liver showed damage to liver cells, when Cisplatin was injected but when Bol or NBol was co-treated with Cisplatin, damage was minimum. Kidney tissue section showed that Cisplatin-alone group moderate glomerular (yellow arrow) and tubular damages (blue arrow), whereas co-treatment group showed almost normal appearance of glomeruli (yellow arrow) and tubules (blue arrow). [(i) = Normal control; (ii) = Cisplatin (10 mg/kg bw); (iii) = Cisplatin (10 mg/kg bw) plus Bol (10 mg/kg bw); (iv) Cisplatin (10 mg/kg bw) plus NBol (10 mg/kg bw)]. (C) Induced-cancerous mice liver sections; there was extensive damage noted in liver tissues of cancer mice. Improvement of histological structure with significantly reduction in liver tissue damage was found in treatment with only Cisplatin and Cisplatin plus Bol/NBol. [(i) = Normal control; (ii) = Cancer mice without treatment; (iii) Cancerous mice with Cisplatin (10 mg/kg bw); (iv) = Cancerous mice with Cisplatin (10 mg/kg bw) plus Bol (10 mg/kg bw); (v) Cancerous mice with Cisplatin (10 mg/kg bw) plus NBol (10 mg/kg bw)].

3.5. Annexin V assay

Cisplatin-treatment caused considerable apoptotic death in normal mice liver cells (83.71%). Co-administration of Bol with Cisplatin and NBol with Cisplatin reduced cell death in normal mice liver cells significantly, by 27.33% for Bol and 56.52% for NBol, respectively, showing NBol to be more efficient by 29.19% as compared to Bol (Fig. 6I). In cancer-induced mice, the % of apoptotic

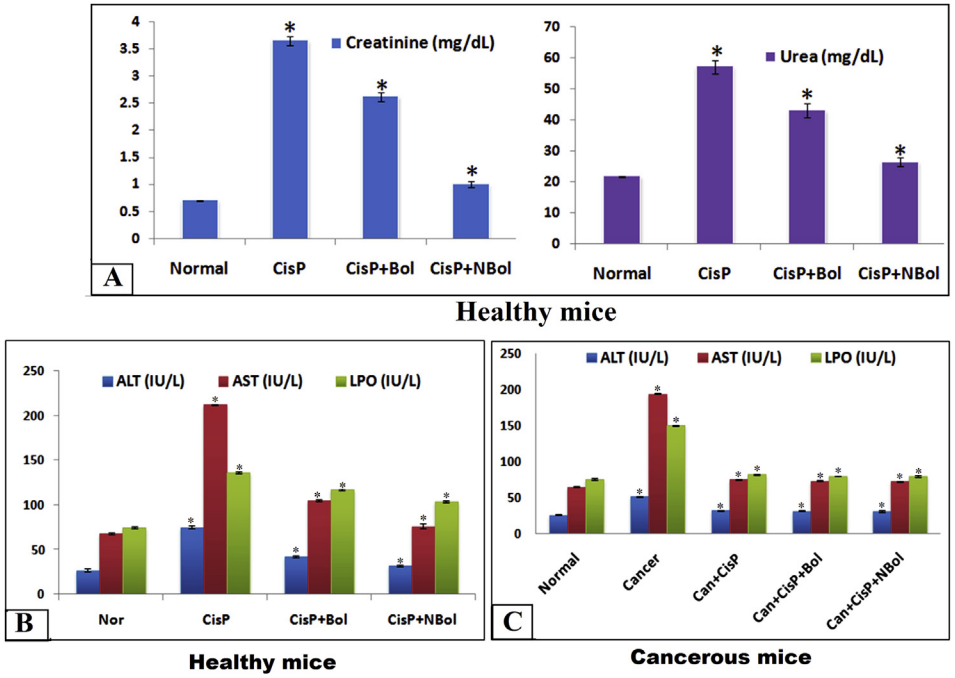

Fig. 5. (A) Bars indicate effect of treatment on creatinine and urea, serum kidney function marker in different groups of normal healthy mice. Effect of treatment on liver function markers (AST, ALT and LPO) in serum of normal healthy (B) and induced-cancerous mice (C). IU/L, international units per litre of the sample; AST, aspartate transaminase; ALT, alanine transaminase; LPO; lipid peroxidation. All data have been expressed in mean ± SE of different samples. *P < 0.05 was considered statistically significant.

Table 1
Mean activities of lipid peroxidation (LPO) (nM/mg protein), glutathione (GSH) (μM/gm) and superoxide dismutase (SOD) (μM/mg protein/min) in kidney and liver of mice of different treated and control group.

	Group 1	Group 2	Group 3	Group 4
Lipid peroxidation (LPO)				
Kidney	1.06 ± 0.078$^{\#}$	5.03 ± 0.097*	3.35 ± 0.120*	2.30 ± 0.126$^{*\#}$
Liver	1.09 ± 0.093$^{\#}$	5.08 ± 0.121	3.27 ± 0.114$^{*\#}$	2.42 ± 0.151$^{*\#}$
Glutathione (GSH)				
Kidney	7.37 ± 0.226$^{\#}$	4.45 ± 0.0132*	5.04 ± 0.032$^{*\#}$	6.08 ± 0.084$^{*\#}$
Liver	6.44 ± 0.197$^{\#}$	2.43 ± 0.009*	3.84 ± 0.054$^{*\#}$	4.82 ± 0.067$^{*\#}$
Superoxide dismutase (SOD)				
Kidney	14.87 ± 0.341$^{\#}$	7.91 ± 0.551*	12.45 ± 0.217$^{*\#}$	14.07 ± 0.314$^{*\#}$
Liver	17.52 ± 0.403$^{\#}$	7.44 ± 0.382	13.33 ± 0.401*	13.26 ± 0.221$^{*\#}$

All values are expressed as mean ± SE. $^{*}P < 0.05$ (for Normal control) and #P < 0.05 (for Cisplatin control) was considered statistically significant. [Group 1 = Normal control; Group 2 = Cisplatin (10 mg/kg bw) control; Group 3 = Cisplatin (10 mg/kg bw) + Boldine (10 mg/kg bw); Group 4 = Cisplatin (10 mg/kg bw) + nano-Boldine (10 mg/kg bw)].

cells was increased, which was significantly reduced in the Cisplatin alone and combined Cisplatin plus Bol/NBol treated mice (Fig. 6II).

3.6. Nuclear changes

Results of TEM study (Fig. 7I and II) revealed an increase in heterochromatin content and clump size, as well as a loss of its characteristic peripheral positioning in Cisplatin alone treatment. But after administration of Cisplatin with Bol/NBol, all changes in chromatin structure became normalized. NBol showed better protective effect than Bol against Cisplatin induced chromatin condensation.

3.7. Quantitative estimation of intracellular ROS generation

Cisplatin treatment caused increase in ROS generation compared to normal control set but co-administration of Cisplatin with either Bol or NBol reduced ROS generation in normal mice liver cells, more prominent in the latter conjoint treatment group (Fig. 7III). ROS generation was increased in the induce cancer mice, which considerably came down after Cisplatin alone treatment as well as in Mice treated combinedly with Cisplatin plus Bol/NBol (Fig. 7IV).

3.8. Quantitative analysis of mitochondrial transmembrane potential (MMP)

Only Cisplatin treatment depolarized MMP in normal cells. Co-administration of Cisplatin with either Bol or NBol reduced depolarization of mitochondria in the normal liver cells. Thus, the conjoint treatment of Cisplatin with NBol yielded better effect to reduce depolarization of MMP in normal liver cell (Fig. 8A). In the induced cancer mice, MMP is depolarized which shows fairly normalized with Cisplatin treatment as well as in combined therapy of Cisplatin plus Bol/NBol (Fig. 8B).

3.9. Change in expression of some key apoptotic genes in both mRNA and protein levels

The analysis of expression at mRNA level revealed that expression of p53, Bax, caspase-3, Cytochrome *c* was up regulated and that of Bcl-2, Top II was down regulated by Cisplatin administration in normal mice liver (Fig. 8C and D). Expression of GAPDH, the housekeeping gene, served as control.

Co-administration of Cisplatin with Bol/NBol suppressed Bax expression and increased Bcl2 expression. The cytochrome *c* translocations also got normalized in the normal mice liver cells. Co-administration of Bol and NBol with Cisplatin tended to decrease p53, caspase 3 activities and increase Top II level towards normal. When the data between Bol and NBol were compared, the latter showed stronger apoptotic effect.

Results of Western Blots and immune-histochemistry have been summarized (Fig. 9A–C). At the protein expression level, expressions of p53, Bax, cytochrome *c* and caspase-3 that favour cytotoxicity were up-regulated in all the cases whereas Bcl-2 and Top II expressions were down-regulated in the only Cisplatin treated cells against GAPDH normalization (Fig. 9A and C). But results from co-treatment group of Cisplatin plus Bol/NBol showed that both Bol and NBol normalized expression of these proteins indicating both Bol and NBol can efficiently work at the gene level to reduce Cisplatin cytotoxicity. NBol showed a greater effect when compared to Bol in this regard.

Increased level of cytochrome *c* into cytosol was further proved by immune-histochemical staining of tissue sections with cytochrome *c* primary antibody by confocal microscopy. Cytochrome *c* expression was increased in the cytosolic fraction in Cisplatin alone treatment group when compared with control. However, in the co-treatment group of Cisplatin with NBol, a significant decrease in the

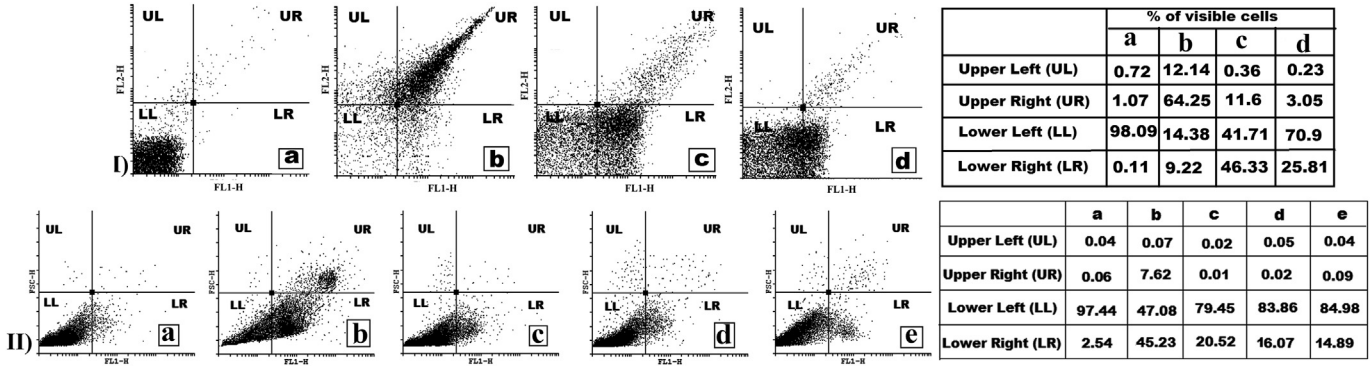

	% of visible cells			
	a	b	c	d
Upper Left (UL)	0.72	12.14	0.36	0.23
Upper Right (UR)	1.07	64.25	11.6	3.05
Lower Left (LL)	98.09	14.38	41.71	70.9
Lower Right (LR)	0.11	9.22	46.33	25.81

	a	b	c	d	e
Upper Left (UL)	0.04	0.07	0.02	0.05	0.04
Upper Right (UR)	0.06	7.62	0.01	0.02	0.09
Lower Left (LL)	97.44	47.08	79.45	83.86	84.98
Lower Right (LR)	2.54	45.23	20.52	16.07	14.89

Fig. 6. Annexin V/PI assay; in normal healthy mice (I) [(Ia) normal mice group, (Ib) only Cisplatin treated group, (Ic) Cisplatin plus Boldine treated group and (Id) Cisplatin plus nano-Boldine treated group] and cancerous mice (II) [(IIa) normal mice group, (IIb) cancerous mice without treatment, (IIc) cancerous mice with only Cisplatin treated, (IIc) cancerous mice with Cisplatin plus Boldine treated and (IId) cancerous mice with Cisplatin plus nano-Boldine treated]. The quadrant of lower left (LL), lower right (LR), upper right (UR) and upper left (UL) show the percentages of live (annexin −ve; PI −ve), early apoptotic (annexin +ve; PI −ve), late apoptotic (annexin +ve; PI +ve) and necrotic cells (PI +ve) respectively.

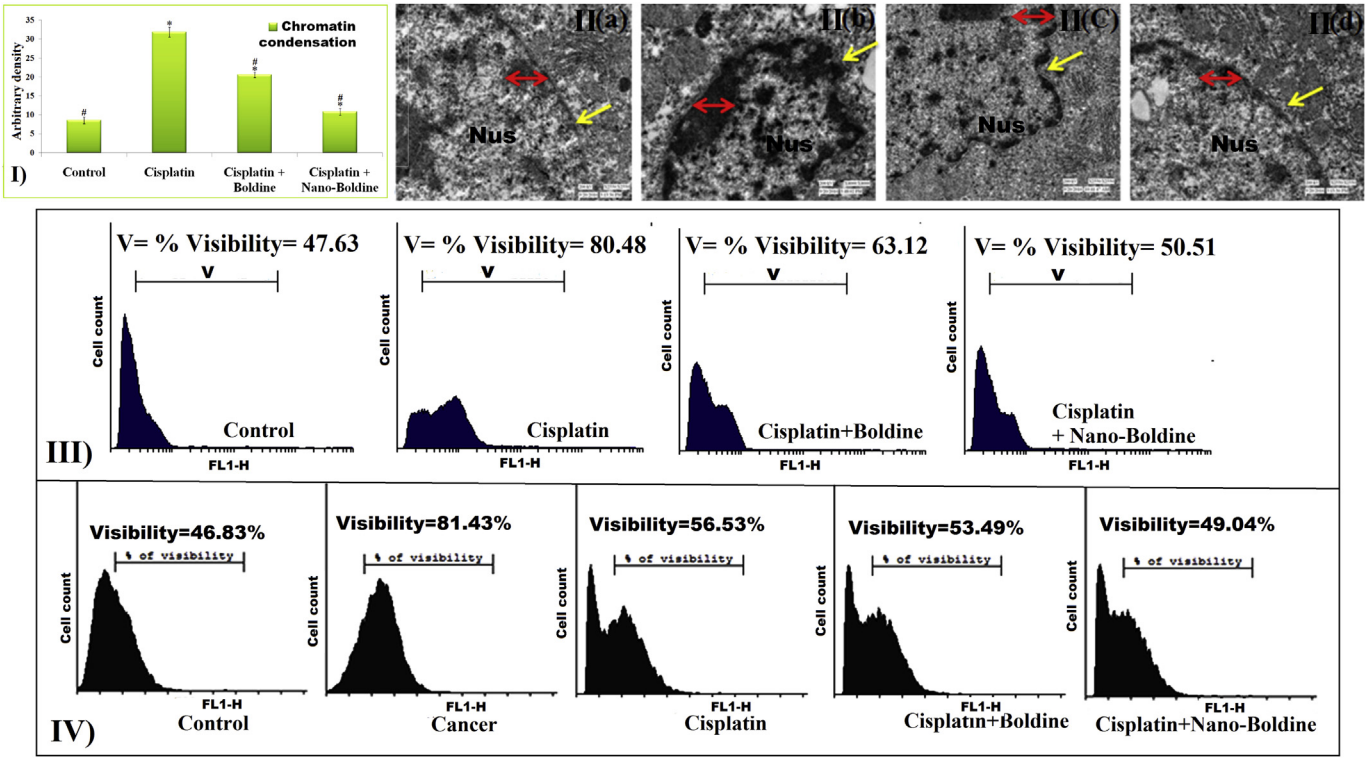

Fig. 7. TEM analysis of liver tissues (I) and (II); representative changes in nuclear organisation like irregular nuclear membrane (marked as yellow arrow) and chromatin condensation (marked as red arrow) after Cisplatin alone treatment as compared to untreated normal mice control but co-administration of Cisplatin with Bol/NBol showed significant reduction in nuclear changes; (IIa) normal without treatment, (IIb) treated with Cisplatin alone, (IIc) Cisplatin plus Boldine co-treatment and (IId) Cisplatin plus nano-Boldine co-treatment. ROS estimation of healthy normal mice (III) and cancerous mice (IV) were determined by flow-cytometry.

up-regulated cytochrome *c* expression in cytosolic fraction was observed (Fig. 9B).

4. Discussion

Results of this study would suggest that in normal mice treated chronically with only Cisplatin for one month, histological analysis of liver tissue revealed extensive tissue damage like cytoplasmic changes, especially around cells of the central vein, hepatocellular vacuolization and sinusoidal dilatations. This would indicate that Cisplatin itself has tissue damaging effect producing toxicity in liver. However, co-administration of Cisplatin and Bol/NBol, brought about significant reduction in liver damage, indicating thereby that both Bol and NBol had potential to protect liver from Cisplatin-induced cytotoxicity in normal mice. The histological examination of kidney in normal mice treated with only Cisplatin also showed remarkable damage in the renal architecture, such as, extensive destruction of tubular space, atrophy of the glomerule and dilatation of urinary space, as compared to that of normal healthy untreated mice. Again, mice receiving the combined therapy demonstrated far less damage in the kidney architecture, indicating thereby the ability of Bol/NBol to protect kidney tissue as well from Cisplatin-induced damage. However, in chronically carcinogen pre-fed mice, there was a tremendous structural damage and degeneration of liver tissue, producing hepato-toxicity, When only Cisplatin was administered to the mice bearing induced liver tumours, the tissue damage was relatively less and some sign of regeneration of damaged tissue was noted. A co-treatment of Bol/NBol to this group of Cisplatin-treated cancer mice also showed tissue regeneration, not showing any antagonistic effect against Cisplatin activity in case of tissue regeneration. In regard to the other parameters of anti-cancer activity, such as, in liver enzymes like ALT, AST, LPO etc, Bol/NBol did not show any effect indicative of reducing Cisplatin anti-cancer action in cancer mice. The mechanistic principle(s) for such phenomenon could not precisely be understood as to why and how NBol tended to protect the normal cells from Cisplatin-induced toxicity, but did not apparently show in case of the cancer cells.

In recent years, nano-technological advances have made it possible to make drug molecules of smaller size and bestowing on them properties suitable for faster entry by encapsulating them in biodegradable nontoxic polymers. This lets them go closer to closer proximity of the target cells and thereby increase their bio-availability. Further, these drug-loaded nano-polymers act as good carriers that allow slow release of the drug at the site of action in the intracellular compartment enhancing the curative efficacy of the drug as well as sustaining its prolonged therapeutic effects [36,37], which is highly solicited. This study revealed that NBol could make the drug more bio-available than could Bol, especially in liver and kidney tissues. Furthermore, NBol had the ability to cross the blood–brain-barrier, presumably because of its much smaller size, suitable negative zeta potential and effective concentration gradient, as evident from its presence in brain tissue, which is a significant finding.

A number of mechanisms have been linked to the development of liver and kidney injury, including glutathione depletion [38], oxidative stress [39], formation of ROS [40] and mitochondrial dysfunction [41]. Cisplatin caused impairment of liver function as indicated by significant increases in serum ALT and AST activities [42]. In the co-treatment series this elevated ALT and AST levels were considerably lowered. Cisplatin administration also produced a significant increase in the levels of serum urea and creatinine which are considered as markers of damage in kidney structure and function of kidney. In the combination treatment group, however,

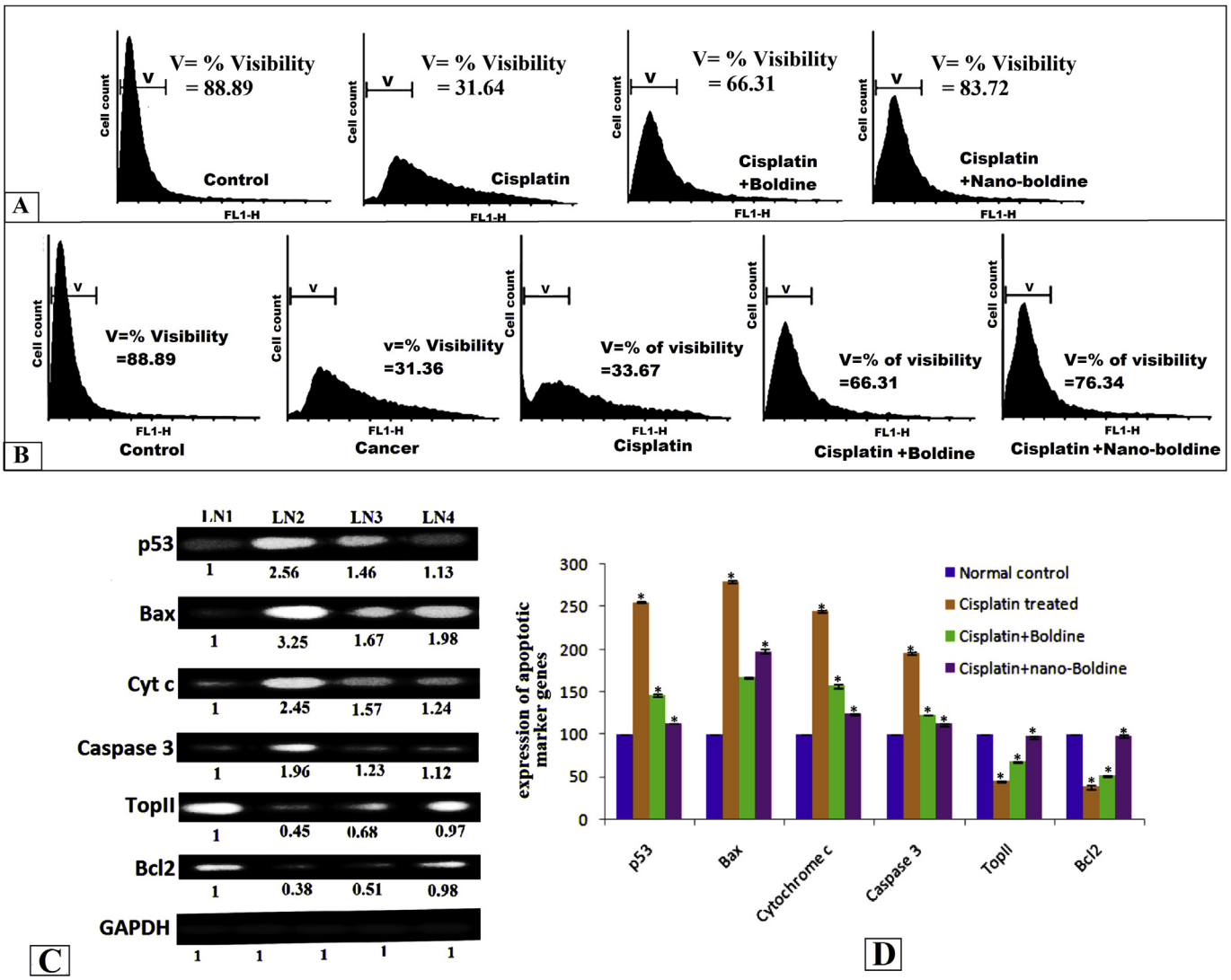

Fig. 8. MMP estimation in normal healthy (A) and cancerous (B) mice were measured by flow-cytometry. (C) RT-PCR analysis of p53, Bax, cytochrome *c*, caspase-3, Bcl-2, and Top II taking GAPDH as housekeeping gene and graphically illustrated in (D). LN1-Normal healthy mice, LN2- Cisplatin (10 mg/kg bw); LN3-Cisplatin (10 mg/kg bw) + Boldine (10 mg/kg bw); LN4- Cisplatin (10 mg/kg bw) + nano-Boldine (10 mg/kg bw). *P < 0.05 was considered statistically significant.

this elevation of marker levels was not observed. Thus, co-treatment of both Bol and NBol provides a protective cover to kidney by impairing/hindering activities of Cisplatin-mediated LPO, and thereby restricting generation of free radical derivatives.

Induction of nephrotoxicity and hepatotoxicity is related to generation of ROS and depletion of GSH level [43]. ROS generated in the cells resulted in the depletion of GSH level, which in turn could further help in Bax translocation from mitochondria to cytosol resulting in induction of apoptosis. In this study, we found that ROS generation was increased along with the reduction in GSH level in the only Cisplatin-treated mice. But ROS level was reduced and GSH level increased when mice were subjected to combined treatment of Bol/NBol and Cisplatin. Additionally, elevated ROS level can also cause damage to DNA, inducing cellular death [44]. Type II topoisomerases (Top II), essential nuclear enzymes, play important roles in DNA replication, transcription, chromosome condensation and de-condensation [45,46]. Down-regulation of Top II expression after only Cisplatin treatment indicated that cells with Cisplatin-produced DNA damage could not proceed towards further divisional activities, and thus pushing cells towards death. In the co-treatment of Cisplatin with Bol/NBol group, expression level of Top-II was near normal. The corresponding expression pattern of p53 also supported this contention. TEM study demonstrated changes like irregular nuclear envelope and chromatin condensation in nuclear organisation occurred after Cisplatin administration, which were fairly not so strikingly damaged in the co-administration group. Cisplatin exposure also caused DNA damage and in the co-treatment, such damage was much less.

CD spectral data suggested that although NBol showed more strong binding with DNA, Bol could not do so at the same level. NBol could enter into the cells more efficiently and faster than Bol; Cisplatin treatment showed a sharp peak shift in reference to CT-DNA, but the peaks observed in the co-treatment group of Cisplatin and Bol/NBol were more towards the normal peaks observed in the control group. This may imply that by some means Bol/NBol prevented active groups of Cisplatin to interact with the CT-DNA and thereby protect from DNA damage caused by Cisplatin. We determined and compared the stability of binding of Bol and NBol with CT-DNA from measurements of Gibb's free energy. Values of ΔG indicated greater spontaneity and binding stability of NBol with DNA.

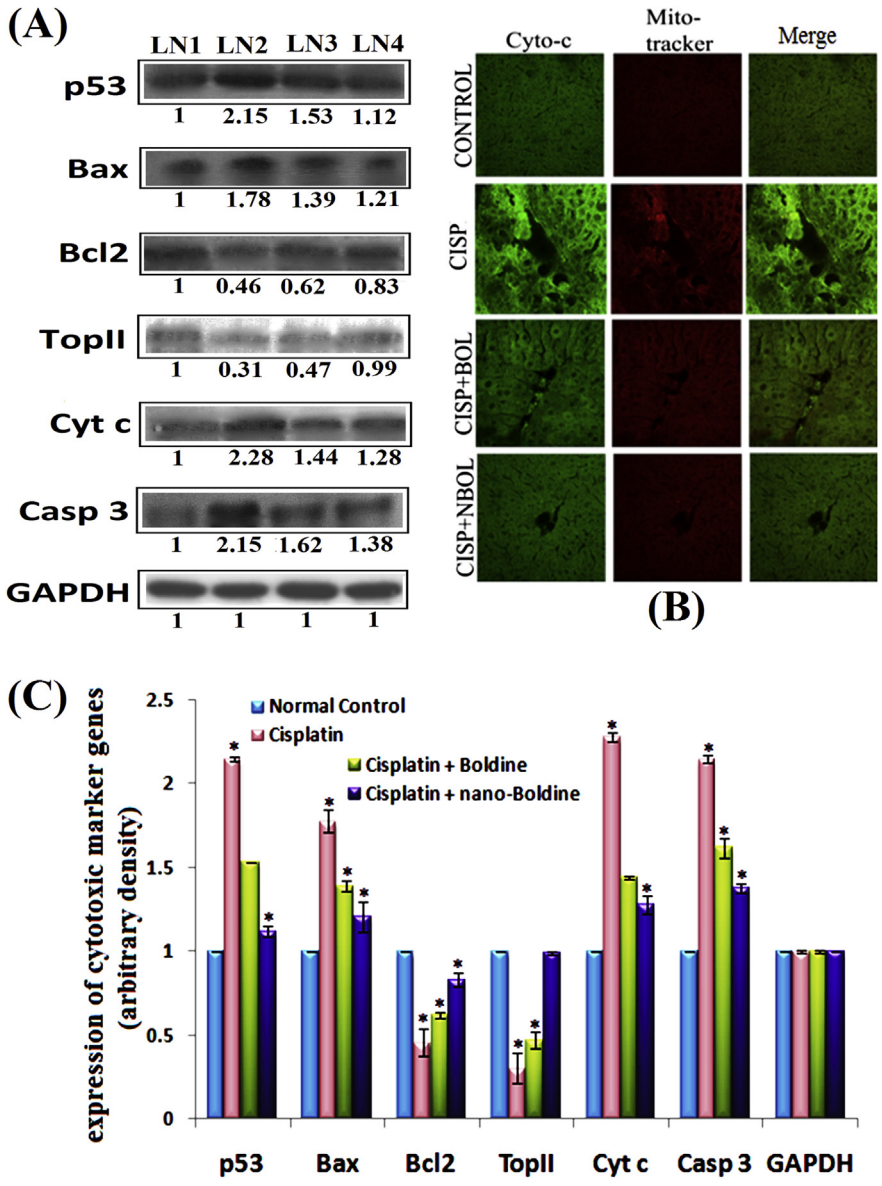

Fig. 9. (A) Immunoblot analysis of p53, Bax, cytochrome *c*, caspase-3, Bcl-2, and Top II taking GAPDH as housekeeping gene. LN1-Normal healthy mice, LN2- Cisplatin (10 mg/kg bw); LN3-Cisplatin (10 mg/kg bw) + Boldine (10 mg/kg bw); LN4- Cisplatin (10 mg/kg bw) + nano-Boldine (10 mg/kg bw). (B) Confocal microscopic analysis of expression and localization of cytochrome *c* in mice tissue section. (C) Graphical protein expression of cytotoxic marker genes of untreated and treated series of mice. *P < 0.05 was considered statistically significant.

To further test whether the reduction of Cisplatin cytotoxicity was activated through changes of cytotoxicity related gene expression [47], we also investigated status of cytochrome *c* release, associated with changes in Bax/Bcl2 protein ratio in only Cisplatin and drug co-treatment groups. Alteration in the level of Bax and Bcl-2 helped us to determine whether cells became cytotoxic and heading towards cell death, or be directed towards normalization. Treatment of Cisplatin alone increased Bax level and decreased Bcl-2 level indicating that cells were directed towards cytotoxic death. On the other hand, the expression levels of Bcl-2 and Bax was found to be only slightly altered in the combined treatment group, particularly in NBol treated group. This observation would suggest that possible molecular mechanism involved through which Bol/NBol reduced cytotoxicity of Cisplatin in normal mice could be through this signalling pathway by controlling Bax/Bcl-2 ratio. This phenomenon was further supported by the level of expressions of cytochrome *c* and caspase-3.

5. Conclusion

Co-administration of Bol/NBol with Cisplatin may be helpful in reducing adversely toxic side effects of Cisplatin therapy. However, more animal experiments may be necessary before recommending the use of this combined therapy in human trials for cancer patients who need and respond well to Cisplatin therapy. In this regard, PLGA polymers as nanocarriers for delivery of drugs appear to be a promising system for several advantages, such as increased protection of encapsulated drug for targeting site-specific localized action [48]. Formulation and usage of the biodegradable nanoparticles render better efficacy, availability, rapid delivery, faster and targeted action in minimum dosage. Further, PLGA has ability to form stable nanoparticles, Therefore, PLGA-loaded NBol appears to have a bright prospect of being used in future drug formulation and effective target-specific delivery for therapeutic use in oncology.

Source of funding

This work was supported by a grant by University of Grant Commission, New Delhi, India, sanctioned to Jesmin Mondal through Maulana Azad National Fellowship scheme vide (sanc.No. F-1-17.1/2012-13/MANF-2012-13-MUS-WES-13662/(SA-III/Website).

Conflict of interest

None.

Acknowledgement

Thanks are also due to Dr. Kajari Ghosh, Department of Chemistry, KU for FTIR spectroscopy. Thanks also go to Dr. Asmita Samadder, Department of Life Science, and JNU for Confocal microscopy. We are grateful to IACS for CD spectroscopy and Dr. T.C. Nag, Department of Anatomy, AIIMS, India for TEM.

Appendix A. Supplementary data

Supplementary data related to this article can be found at https://doi.org/10.1016/j.jaim.2017.11.002.

References

[1] World Health Organization. WHO model list of essential medicines (19th list). April 2015. Retrieved 8 December 2016, http://www.who.int/medicines/publications/essentialmedicines/EML2015_8-May-15.pdf.
[2] Hanigan MH, Devarajan P. Cisplatin nephrotoxicity: molecular mechanisms. Cancer Ther 2003;1:47–61.
[3] Lu Y, Cederbaum AI. Cisplatin-induced hepatotoxicity is enhanced by elevated expression of cytochrome P450 2E1. Toxicol Sci 2006;89:515–23.
[4] Amptoulach S, Tsavaris N. Neurotoxicity caused by the treatment with platinum analogues. Chemother Res Pract 2011;2011:843019.
[5] Ishida S, Lee J, Thiele DJ, Herskowitz I. Uptake of the anticancer drug cisplatin mediated by the copper transporter Ctr1 in yeast and mammals. Proc Natl Acad Sci USA 2002;99:14298–302.
[6] Cohen SM, Lippard SJ. Cisplatin: from DNA damage to cancer chemotherapy. Prog Nucleic Acid Res Mol Biol 2001;67:93–130.
[7] Nazıroglua M, Karaoğlub A, Aksoy AO. Selenium and high dose vitamin E administration protects cisplatin-induced oxidative damage to renal, liver and lens tissues in rats. Toxicology 2004;195:221–30.
[8] Işeri S, Ercan F, Gedik N, Yüksel M, Alican I. Simvastatin attenuates cisplatin-induced kidney and liver damage in rats. Toxicology 2007;230:256–64.
[9] Chirinoa YI, Pedraza-Chaverri J. Role of oxidative and nitrosative stress in cisplatin-induced nephrotoxicity. Exp Toxicol Pathol 2009;61:223–42.
[10] Yüce A, Ateşşahin A, Ceribaşi AO, Aksakal M. Ellagic acid prevents cisplatin-induced oxidative stress in liver and heart tissue of rats. Basic Clin Pharmacol Toxicol 2007;101:345–9.
[11] Florea AM, Büsselberg D. Cisplatin as an anti-tumor drug: cellular mechanisms of activity, drug resistance and induced side effects. Cancers (Basel) 2011;3:1351–71.
[12] Nagothu KK, Bhatt R, Kaushal GP, Portilla D. Fibrate prevents cisplatin-induced proximal tubule cell death. Kidney Int 2005;68:2680–93.
[13] Zhou W, Kavelaars A, Heijnen CJ. Metformin prevents cisplatin-induced cognitive impairment and brain damage in mice. PLoS One 2016;11, e0151890.
[14] Lau YS, Ling WC, Murugan D, Mustafa MR. Boldine ameliorates vascular oxidative stress and endothelial dysfunction: therapeutic implication for hypertension and diabetes. J Cardiovasc Pharmacol 2015;65:522–31.
[15] Youn YC, Kwon OS, Han ES, Song JH, Shin YK, Lee CS. Protective effect of boldine on dopamine- induced membrane permeability transition in brain mitochondria and viability loss in PC12 cells. Biochem Pharmacol 2002;63:495–505.
[16] Vasir JK, Labhasetwar V. Biodegradable nanoparticles for cytosolic delivery of therapeutics. Adv Drug Deliv Rev 2007;59:718–28.
[17] Lü J, Wang X, Marin-Muller C, Wang H, Lin PH, Yao Q, et al. Current advances in research and clinical applications of PLGA-based nanotechnology. Expert Rev Mol Diagn 2009;9:325–41.
[18] Danhiera F, Ansorenaa E, Silvaa JM, Cocoa R, Bretona AL, Préata V. PLGA-based nanoparticles: an overview of biomedical applications. J Control Release 2012;161:505–22.
[19] Samadder A, Das J, Das S, De A, Saha SK, Bhattacharyya SS, et al. Poly(lactic-co-glycolic) acid loaded nano-insulin has greater potentials of combating arsenic induced hyperglycemia in mice: some novel findings. Toxicol Appl Pharmacol 2013;267:57–73.
[20] Hines DJ, Kaplan DL. Poly (lactic-co-glycolic acid) controlled release systems: experimental and modeling insights. Crit Rev Ther Drug Carrier Syst 2013;30:257–76.
[21] Mondal J, Bishayee K, Panigrahi AK, Khuda-Bukhsh AR. Low doses of ethanolic extract of Boldo (*Peumus boldus*) can ameliorate toxicity generated by cisplatin in normal liver cells of mice in vivo and in WRL-68 cells in vitro, but not in cancer cells in vivo or in vitro. J Integr Med 2014;12:425–38.
[22] Mondal J, Panigrahi AK, Khuda-Bukhsh AR. Physico-chemical and ultra-structural characterizations of PLGA-loaded nanoparticles of Boldine and their efficacy in ameliorating cisplatin induced hepatotoxicity in normal liver cells in vitro. JIPBS 2015;2:506–21.
[23] Fessi H, Puisieux F, Devissaquet JP, Ammoury N, Benita S. Nanocapsule formation by interfacial polymer deposition following solvent displacement. Int J Pharm 1989;55:1–4.
[24] Park TG, Lu W, Crotts G. Importance of in vitro experimental conditions on protein release kinetics, stability and polymer degradation in protein encapsulated poly (d,l-lactic acid-co-glycolic acid) microspheres. J Control Release 1995;33:211–22.
[25] Banik M, Basu T. Calcium phosphate nanoparticles: a study of their synthesis, characterization and mode of interaction with salmon testis DNA. Dalton Trans 2014;43:3244–59.
[26] Dominguez MF, Macias RI, Izco-Basurko I, de La Fuente A, Pascual MJ, Criado JM, et al. Low in vivo toxicity of a novel Cisplatin-ursodeoxycholic derivative (Bamet-UD2) with enhanced cytostatic activity versus liver tumors. J Pharmacol Exp Ther 2001;297:1106–12.
[27] Mosmann T. Rapid colorimetric assay for cellular growth and survival: application to proliferation and cytotoxicity assays. J Immunol Methods 1983;65:55–63.
[28] Ohkawa H, Ohishi N, Yagi K. Assay for lipid peroxidation in animal tissues by thiobarbituric acid reaction. Anal Biochem 1979;95:351–8.
[29] Sedlak J, Lindsay RH. Estimation of total, protein-bound, and nonprotein sulfhydryl groups in tissue with Ellman's reagent. Anal Biochem 1968;25:192–205.
[30] Kakkar P, Das B, Viswanathan PN. A modified spectrophotometric assay of superoxide dismutase. Indian J Biochem Biophys 1984;21:130–2.
[31] Schumann G, Bonora R, Ceriotti F, Férard G, Ferrero CA, Franck PF, et al. International federation of clinical Chemistry and laboratory medicine. Clin Chem Lab Med 2002;40:725–33.
[32] Chakraborty D, Samadder A, Dutta S, Khuda-Bukhsh AR. Antihyperglycemic potentials of a threatened plant, Helonias dioica: antioxidative stress responses and the signalling cascade. Exp Biol Med 2012;237:64–76 (a).
[33] Cherkezyan L, Stypula-Cyrus Y, Subramanian H, White C, Cruz MD, Wali RK, et al. Nanoscale changes in chromatin organization represents the initial steps of tumorigenesis: a transmission electron microscopy study. BMC Cancer 2014;14:189.
[34] Dhiman R, Kathania M, Raje M, Majumder S. Inhibition of bf1-1/A1 by SiRNA inhibits mycobacterial growth in THP-1 cells by enhancing phagosomal acidification. Biochim Biophys Acta 2008;1780:733–42.
[35] Burnette WN. "Western blotting": electrophoretic transfer of proteins from sodium dodecyl sulfate-polyacrylamide gels to unmodified nitrocellulose and radiographic detection with antibody and radio iodinated protein. Anal Biochem 1981;112:195–203.
[36] Suh H, Jeong B, Rathi R, Kim SW. Regulation of smooth muscle cell proliferation using paclitaxel-loaded poly(ethylene oxide)-poly(lactide/glycolide) nanospheres. J Biomed Mater Res A 1998;42:331–8.
[37] Panyam J, Zhou WZ, Prabha S, Sahoo SK, Labhasetwar V. Rapid endolysosomal escape of poly (d,l-lactide-co-glycolide) nanoparticles: implications for drug and gene delivery. FASEB J 2002;16:1217–26.
[38] Miller RP, Tadagavadi RK, Ramesh G, Reeves WB. Mechanisms of cisplatin nephrotoxicity. Toxins (Basel) 2010;2:2490–518.
[39] Jaeschke H, Knight TR, Bajt ML. The role of oxidant stress and reactive nitrogen species in acetaminophen hepatotoxicity. Toxicol Lett 2003;144:279–88.
[40] Agarwal R, MacMillan-Crow LA, Rafferty TM, Saba H, Roberts DW, Fifer EK, et al. Acetaminophen-induced hepatotoxicity in mice occurs with inhibition of activity and nitration of mitochondrial manganese superoxide dismutase. J Pharmacol Exp Ther 2011;337:110–8.
[41] Kon T, Nishiura M, Ohkura R, Toyoshima YY, Sutoh K. Distinct functions of nucleotide-binding/hydrolysis sites in the four AAA modules of cytoplasmic dynein. Biochemistry 2004;43:11266–74.
[42] Ghouri N, Preiss D, Sattar N. Liver enzymes, nonalcoholic fatty liver disease, and incident cardiovascular disease: a narrative review and clinical perspective of prospective data. Hepatology 2010;52:1156–61.
[43] Battin EE, Brumaghim JL. Antioxidant activity of sulfur and selenium: a review of reactive oxygen species scavenging, glutathione peroxidase, and metal-binding antioxidant mechanisms. Cell Biochem Biophys 2009;55:1–23.

[44] Rowe LA, Degtyareva N, Doetsch PW. DNA damage-induced reactive oxygen species (ROS) stress response in Saccharomyces cerevisiae. Free Radic Biol Med 2008;45:1167–77.
[45] Goodsell DS. The molecular perspective: DNA topoisomerases. Stem Cell Res 2002;20:470–1.
[46] Wang JC. Cellular roles of DNA topoisomerases: a molecular perspective. Nat Rev Mol Cell Biol 2002;3:430–40.
[47] Bhatt K, Zhou L, Mi QS, Huang S, She JX, Dong Z. MicroRNA-34a is induced via p53 during cisplatin nephrotoxicity and contributes to cell survival. Mol Med 2010;16:409–16.
[48] Zhang Z, Tsai PC, Ramezanli T, Michniak-Kohn BB. Polymeric nanoparticles-based topical delivery systems for the treatment of dermatological diseases. Wiley Interdiscip Rev Nanomed Nanobiotechnol 2013;5:205–18.